

Dynamics of carrier injection through V-defects in long wavelength GaN LEDs

Cite as: Appl. Phys. Lett. **124**, 181108 (2024); doi: [10.1063/5.0206357](https://doi.org/10.1063/5.0206357)

Submitted: 1 March 2024 · Accepted: 23 April 2024 ·

Published Online: 1 May 2024



View Online



Export Citation



CrossMark

Saulius Marcinkevicius,^{1,a)} Tanay Tak,² Yi Chao Chow,² Feng Wu,² Rinat Yapparov,¹
Steven P. DenBaars,² Shuji Nakamura,² and James S. Speck²

AFFILIATIONS

¹Department of Applied Physics, KTH Royal Institute of Technology, AlbaNova University Center, 10691 Stockholm, Sweden

²Materials Department, University of California, Santa Barbara, California 93106, USA

^{a)} Author to whom correspondence should be addressed: sm@kth.se

ABSTRACT

The efficiency of high-power operation of multiple quantum well (QW) light emitting diodes (LEDs) to a large degree depends on the realization of uniform hole distribution between the QWs. In long wavelength InGaN/GaN QW LEDs, the thermionic interwell hole transport is hindered by high GaN barriers. However, in polar LED structures, these barriers may be circumvented by the lateral hole injection via semipolar {10 $\bar{1}$ 1} QWs that form on the facets of V-defects. The efficiency of such carrier transfer depends on the transport time since transport in the semipolar QWs is competed by recombination. In this work, we study the carrier transfer from the semipolar to polar QWs by time-resolved photoluminescence in long wavelength (green to red) LEDs. We find that the carrier transfer through the semipolar QWs is fast, a few tens of picoseconds with the estimated room temperature ambipolar diffusion coefficient of ~ 5.5 cm²/s. With diffusion much faster than recombination, the hole transport from the *p*-side of the structure to the polar QWs should proceed without a substantial loss, contributing to the high efficiency of long wavelength GaN LEDs.

© 2024 Author(s). All article content, except where otherwise noted, is licensed under a Creative Commons Attribution (CC BY) license (<https://creativecommons.org/licenses/by/4.0/>). <https://doi.org/10.1063/5.0206357>

Long wavelength (green to red) InGaN/GaN quantum well (QW) light emitting diodes (LEDs) and micro-LEDs are essential components of solid-state lighting and displays based on the GaN material system. However, efficiency of these devices is inferior to their blue-emitting counterparts.¹ In addition, efficiency of high-power devices based on multiple QWs is affected by the poor interwell hole transport and resulting nonuniform carrier distribution between the QWs.^{2–5} Carrier accumulation in the QW closest to the *p*-side of an LED would increase the nonradiative Auger recombination and cause efficiency droop,^{3,6} while QWs on the *n*-side of the structure would have a low hole population, enhanced Shockley–Read–Hall recombination, and small contribution to the overall emission. Thus, to reach a high efficiency in multiple QW LEDs operating at large drive currents, a uniform interwell carrier distribution is required.

Lateral carrier injection from the sides of the QWs has been suggested as means to achieve such a uniform distribution.⁷ However, efficiency of the lateral injection is reduced by the poor carrier diffusion in the QW plane, surface recombination, and current leakage.⁸ So far, the most efficient scheme of the lateral hole injection seems to be via semipolar QWs formed on the sidewalls of V-defects in polar InGaN QW

structures.^{9,10} The V-defects typically form at threading dislocations under conditions of kinetically limited growth and have shapes of inverted hexagonal pyramids with semipolar {10 $\bar{1}$ 1} sidewall planes.¹¹ In QW structures, both polar (0001) QWs and semipolar {10 $\bar{1}$ 1} QWs on the facets of the V-defects are present. The thickness and indium content of the semipolar QWs are much smaller than of the polar ones increasing energy of the electron and hole ground levels with respect to the polar QWs.^{12–14} The shallow valence band potential of the semipolar QWs enables hole injection from the *p*-side of the structure into all semipolar QWs with the subsequent transfer to the polar ones. The V-defect carrier injection has explicitly been studied by theoretical modeling,¹⁵ and measurements of luminescence,¹⁶ and electron emission microscopy.¹⁷ However, the efficiency and velocity of the carrier transfer via the semipolar QWs are yet unknown. If the injected hole transport time to the polar QWs were long, the transfer efficiency would be rivaled by recombination in the semipolar QWs reducing efficiency of the hole transfer. In this work, we explore this effect by optical studies of carrier dynamics in the semipolar sidewall QWs.

Experiments were performed by time-resolved photoluminescence (PL) on long wavelength (550–600 nm) single and multiple QW

LEDs. The structures were grown by metalorganic chemical vapor deposition on *c*-plane sapphire substrates. They consisted of an unintentionally doped GaN template layer, *n*-GaN layer, 20-period 2.2 nm/4.5 nm *n*-In_{0.04}Ga_{0.96}N/GaN superlattice serving to reduce the point defect density and generate V-defects, 30 nm *n*-GaN layer, active region, *p*-Al_{0.10}Ga_{0.90}N electron blocking layer, and *p*- and *p*⁺-GaN contact layers. The active region contained either one or five 2.4–3.6 nm thick InGaN QWs followed by a 2 nm Al_{0.10}Ga_{0.90}N capping layer and 13 nm GaN barrier. The In content in the QWs was between 0.22 and 0.26, as determined by cross-sectional high angle annular dark field scanning transmission electron microscopy (HAADF-STEM) and energy-dispersive x-ray spectroscopy (EDS). More details on the studied structures can be found in Ref. 18. PL dynamics did not show any major dependence on the number of QWs, their thickness, or composition. Hence, the work is focused on the LED with five 2.5 nm In_{0.27}Ga_{0.73}N/GaN QWs in the active region.

PL dynamics of the sidewall QWs was measured using second harmonic pulses (200 fs pulse duration, 76 MHz pulse repetition frequency) of a Ti:sapphire laser for excitation and a spectrometer/streak camera system for detection. PL decay times of the polar QWs were much longer than the pulse period; hence, for these measurements, the pulse repetition rate was reduced to 4 MHz with a pulse picker, and PL dynamics was recorded with a time-correlated single photon counter. The excitation wavelength of 390 nm was below the GaN bandgap exciting carriers only in the QWs. The measurements were performed in the temperature range from 7 to 293 K at pulse energies between 13 and 650 pJ, which corresponds to photoexcited carrier densities directly after a pulse between 1×10^{16} and $5 \times 10^{17} \text{ cm}^{-3}$. In this estimation, a laser spot diameter of 50 μm , GaN reflectivity of 0.15, and InGaN absorption coefficient of $1 \times 10^4 \text{ cm}^{-1}$ were used.

Figure 1(a) shows a HAADF-STEM image of the five 2.5 nm In_{0.27}Ga_{0.73}N/GaN QW structure in the vicinity of a V-defect. One side of a semipolar QW merges with a polar one while the other side is terminated by a threading dislocation (TD). Atom probe tomography studies by Yamaguchi *et al.*¹⁴ have revealed that within a few nm around the dislocation the indium content is about twice as high as in the polar QW. We expect that in our samples it is ~ 0.5 , which can also be judged from the high contrast between the TD region and QW layers in the HAADF-STEM image. The well width and indium

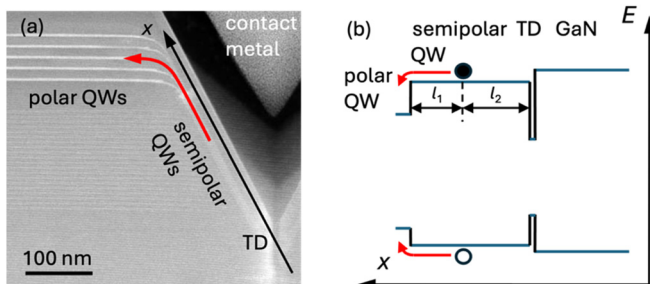


FIG. 1. Cross-sectional HAADF-STEM image of a five QW structure in the vicinity of a V-defect. The red arrow shows the path of the carrier transport from the semipolar to polar QWs (a). Schematic band diagram in the direction of the semipolar QW plane (b). TD indicates a threading dislocation, and l_1 and l_2 denote lengths of the semipolar QW segments from which photoexcited carriers are trapped either to the polar QW or TD-related traps.

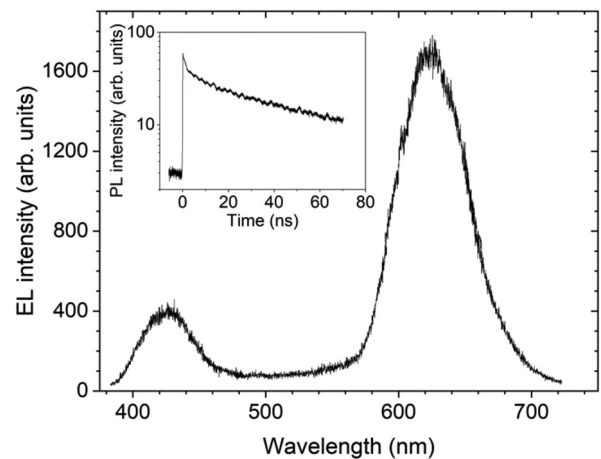


FIG. 2. Room temperature EL spectrum. The inset shows PL dynamics of the polar QW peak.

content in the semipolar QWs are 2.0 nm and 0.07, respectively, as determined by HAADF-STEM and EDS.¹⁸

Figure 2 shows a room temperature EL spectrum with peaks at 610 and 427 nm, which, following energy level calculations and confocal micro-PL measurements of Ref. 18, can be assigned to the ground state transitions in the polar and semipolar QWs. The PL decay time of the polar QW peak (inset to Fig. 2) is 47 ns. PL dynamics of the semipolar QWs is much faster (Fig. 3). The decay transient has a double-exponential shape with the prevailing short component of 20–40 ps and the long component in the range of 0.5–1 ns. One should note that 390 nm pulses excite carriers in both polar and semipolar QWs. However, since the intraband carrier relaxation in nitrides occurs on a sub-picosecond timescale (beyond the resolution of the streak camera),¹⁹ the transients of Fig. 3 reflect the carrier dynamics in the semipolar QWs. The long PL decay component is most probably determined by the recombination of carriers localized at band potential

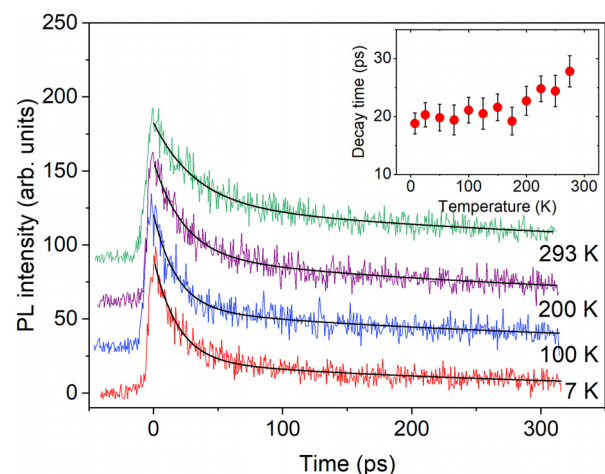


FIG. 3. PL transients for the semipolar QWs at different temperatures. The inset shows temperature dependence of the fast decay time.

fluctuations. Its duration is similar to PL decay times of 1–2 ns observed in homoepitaxially grown semipolar InGaN QWs.²⁰ The short PL decay component might have two possible origins: a fast carrier trapping to traps and/or recombination centers or carrier transport from the semipolar to polar QWs and TDs. The first possibility is rather unlikely because the short trapping times would require large trap or recombination center concentrations. Trapping times of the order of 1–10 ps have been observed in proton-implanted or Fe-doped GaN, however, only for defect or impurity concentrations of the order of $1 \times 10^{19} \text{ cm}^{-3}$.^{21–23} Our QWs are neither doped with deep traps nor treated to enhance the point defect concentration. Nevertheless, to definitely prove or disapprove that the fast component reflects the photoexcited carrier transfer, an investigation of the PL dynamics at different temperatures and excitation powers was performed.

The semipolar QW PL transients at several temperatures are shown in Fig. 3. The fast decay times are gathered in the inset. The decay times are similar up to $\sim 200 \text{ K}$; at higher temperatures they experience a moderate increase. This temperature dependence of the short PL decay times allows distinguishing the mechanism that is responsible for the fast decay component.

For the ultrafast carrier trapping, the PL decay time is defined by the time of minority carrier trapping and/or nonradiative SRH recombination. The carrier trapping rate of electrons or holes is expressed as $1/\tau_{NRe,h} = C_{e,h}N_{e,h} = \bar{v}_{e,h}\sigma_{e,h}N_{e,h}$, where $N_{e,h}$ is the trap concentration, $C_{e,h}$ is the trapping coefficient, $\bar{v}_{e,h}$ is the thermal velocity, and $\sigma_{e,h}$ is the capture cross section. Calculations show that at low temperatures the trapping process is determined by tunneling and is temperature independent.²⁴ In the high temperature regime ($\geq 150 \text{ K}$), the trapping time decreases with increasing temperature because of the thermal activation of traps. This is an opposite trend to what we observe for the semipolar QW PL decay times. In addition, the trapping times would increase with increased excitation power due to a partial filling of the traps.²⁵ The short semipolar QW decay times in the used pulse energy range do not depend on the excitation level, contradicting the trapping hypothesis.

On the other hand, if the carrier dynamics in the semipolar QWs were governed by the carrier transfer, the PL decay time would be determined by diffusion with the polar QWs and, possibly, TDs acting as carrier sinks [Fig. 1(b)].^{26,27} At zero bias used in the time-resolved PL measurements of Fig. 3, the semipolar QWs are not populated, and photoexcited carrier diffusion is ambipolar governed by the slower holes, $D_{amb} \approx 2D_h$.

In bulk GaN, the hole diffusion coefficient D_h at high temperatures decreases because of an increased rate of the acoustic and polar optical phonon scattering.²⁸ In QWs, the temperature independent interface scattering is also an important scattering mechanism, especially in narrow QWs²⁹ with rather diffuse well/barrier interfaces.^{13,30} Assuming that the PL decay time is determined by the carrier transfer, at first glance, the fast low temperature diffusion might seem surprising. The linear dependence of the diffusion coefficient on temperature [$D_h = \mu_h kT/e$, where μ_h is the hole mobility, k is the Boltzmann constant, T is the lattice temperature, and e is the elementary charge] would imply that at low temperatures the diffusion should cease. Such effect has been observed in optical studies of carrier diffusion in single InGaN QWs without a carrier sink.³¹ One should bear in mind, however, the different time scales of diffusion in extended planar QWs^{31–33} and diffusion over short distances in structures with a carrier sink.

In the planar QWs, the diffusion proceeds during the carrier lifetime, which may be of the order of 100 ns to μs . In our case, the carrier transport takes just a few tens of picoseconds. During that time, photoexcited carriers remain hot; a full thermalization with the lattice occurs on the 100 ps scale.¹⁹ Thus, it is not surprising that most holes are mobile even at low lattice temperatures, which is also consistent with the weak temperature dependence of the transfer time. A certain increase in this time at high temperatures suggests that at these conditions the phonon scattering prevails the interface scattering.

The temperature dependence of the semipolar QW PL decay times and other above-mentioned given arguments allow assigning the fast PL decay component to the carrier transfer. However, estimation of the diffusion parameters is not trivial because it depends on the efficiency of the carrier sinks on both sides of the semipolar QW, namely, the polar QW and TD. The inset to Fig. 4 shows estimation of the ambipolar diffusion coefficient for different fractions of carriers [or lengths l_1 and l_2 , Fig. 1(b)] diffusing toward the polar QW and TD. The estimation was made by solving a one-dimensional diffusion equation $\partial N(x, t)/\partial t = D_{amb}\partial^2 N(x, t)/\partial x^2$, where N is the number of the electron hole pairs and τ is the transport time. In the calculation, recombination in the semipolar QW has been neglected because the recombination time is much longer than the transport time. The length of the semipolar QW was taken as 320 nm [Fig. 1(a)], and boundaries of the semipolar QW with the polar QW and TD were assumed as ideal sinks, i.e., at these points $N = 0$.

To make a realistic estimate of $l_2/(l_1 + l_2)$, one should analyze the carrier trapping in the TD region. First, one should note that within a few nm around the dislocation the indium content in the alloy is ~ 5 times larger than in the semipolar QW.¹⁴ Such small inclusions of a high In content material resemble quantum dots. Because of the low band potentials, the quantum dot ground levels should have smaller energies than the semipolar QW bands allowing to capture carriers from the QW. However, the density of states in the quantum dots is small, and these states could be easily filled, especially under forward bias. The state filling would eliminate the high indium content regions as carrier sinks leaving SRH recombination at

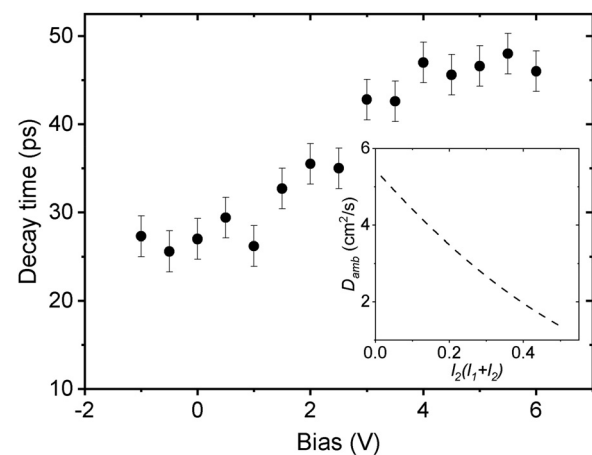


FIG. 4. Dependence of the PL decay time on bias at room temperature. The inset shows dependence of the ambipolar diffusion coefficient on the relative length of the semipolar QW region from which carriers are trapped to the TD traps.

dislocation-related point defects as the main channel of the carrier removal from the semipolar QW at the TD end.

The impact of this SRH recombination can be reduced by filling the traps under positive bias, just like it is reduced in LEDs at medium to high currents. The bias dependence of the PL decay time is shown in Fig. 4. One can notice that between 0 and 6 V the decay time first increases and then saturates. The saturation occurs at about 4 V corresponding to the current density of $\sim 20 \text{ A/cm}^2$. At this current, the TD-related traps are filled, and the carrier sink at TDs is eliminated. Then, the majority of photoexcited carriers (except for those recombining in the semipolar QWs) would transfer to the polar QWs yielding $l_2/(l_1 + l_2) \approx 0$ and $D_{amb} \approx 5.5 \text{ cm}^2/\text{s}$. At zero bias, the PL decay time is smaller by a factor of 1.5. For the same diffusion coefficient, this reduces the effective length for the carrier transfer into the polar QWs by 1.2 showing that even at zero bias the carrier trapping to the polar QWs is more efficient than to the TD-related point defects.

The estimated ambipolar diffusion coefficient is larger than previously reported room temperature values for InGaN QWs ($0.25\text{--}1.9 \text{ cm}^2/\text{s}$).^{31,34,35} The most probable reason for this high value is the presence of the carrier sink in the form of the polar QWs.

In conclusion, the time-resolved PL measurements of carrier dynamics in the semipolar QWs at the V-defect facets have shown that the carrier transfer to the polar QWs is fast, a few tens of picoseconds. With diffusion being nearly several orders of magnitude faster than recombination, the hole transport from the *p*-side of the structure to the polar QWs should proceed without a substantial loss and contribute to the high efficiency of long wavelength GaN LEDs.

The research at KTH has been financially supported by the Swedish Energy Agency (Project No. P2022-00251) and the Swedish Research Council (Project No. 2023-03538). The support at UCSB was provided by the Solid State Lighting and Energy Electronics Center (SSLEEC); U.S. Department of Energy under the Office of Energy Efficiency & Renewable Energy (EERE) Award Nos. DE-EE0009691; the National Science Foundation (NSF) RAISE program (Grant No. DMS-1839077); the Simons Foundation (Grant No. 601952 for J.S.S.); and the Sandia National Laboratory (Grant No. 2150283). T.T. acknowledges the Department of Defense's National Defense Science and Engineering Graduate Fellowship for their support.

AUTHOR DECLARATIONS

Conflict of Interest

The authors have no conflicts to disclose.

Author Contributions

Saulius Marcinkevičius: Conceptualization (lead); Formal analysis (lead); Funding acquisition (equal); Investigation (lead); Resources (equal); Visualization (lead); Writing – original draft (lead); Writing – review & editing (lead). **Tanay Tak:** Conceptualization (supporting); Investigation (supporting); Resources (equal); Writing – review & editing (supporting). **Yi Chao Chow:** Resources (equal). **Feng Wu:** Data curation (equal); Formal analysis (equal); Investigation (supporting); Visualization (supporting). **Rinat Yapparov:** Formal analysis (equal); Investigation (supporting); Visualization (supporting). **Steven P. DenBaars:** Funding acquisition (equal); Resources (supporting).

Shuji Nakamura: Funding acquisition (equal); Resources (supporting). **James S. Speck:** Funding acquisition (equal); Resources (equal); Supervision (lead); Writing – review & editing (supporting).

DATA AVAILABILITY

The data that support the findings of this study are available from the corresponding author upon reasonable request.

REFERENCES

- Z. Zhuang, D. Iida, and K. Ohkawa, *Jpn. J. Appl. Phys., Part 1* **61**, SA0809 (2022).
- A. David, M. J. Grundmann, J. F. Kaeding, N. F. Gardner, T. G. Mihopoulos, and M. R. Krames, *Appl. Phys. Lett.* **92**, 053502 (2008).
- P. Liu, J.-H. Ryou, R. D. Dupuis, J. Han, G. D. Shen, and H. B. Wang, *Appl. Phys. Lett.* **93**, 021102 (2008).
- W. G. Scheibenzuber and U. T. Schwarz, *Appl. Phys. Express* **5**, 042103 (2012).
- S. Marcinkevičius, R. Yapparov, L. Y. Kuritzky, Y.-R. Wu, S. Nakamura, S. P. DenBaars, and J. S. Speck, *Appl. Phys. Lett.* **114**, 151103 (2019).
- J.-Y. Chang, Y.-A. Chang, T.-H. Wang, F.-M. Chen, B.-T. Liou, and Y.-K. Kuo, *Opt. Lett.* **39**, 497 (2014).
- P. Kivisaari, J. Oksanen, and J. Tulkki, *J. Appl. Phys.* **111**, 103120 (2012).
- D. Schiavon, M. Chlipala, and P. Perlin, *Opt. Express* **29**, 3001 (2021).
- F. Jiang, J. Zhang, L. Xu, J. Ding, G. Wang, X. Wu, X. Wang, C. Mo, Z. Quan, X. Guo, C. Zheng, S. Pan, and J. Liu, *Photonics Res.* **7**, 144 (2019).
- S. Zhang, J. Zhang, J. Gao, X. Wang, C. Zheng, M. Zhang, X. Wu, L. Xu, J. Ding, Z. Quan, and F. Jiang, *Photonics Res.* **8**, 1671 (2020).
- X. H. Wu, C. R. Elsass, A. Abare, M. Mack, S. Keller, P. M. Petroff, S. P. DenBaars, J. S. Speck, and S. J. Rosner, *Appl. Phys. Lett.* **72**, 692 (1998).
- C. Netzel, H. Bremers, L. Hoffmann, D. Fuhrmann, U. Rossow, and A. Hangleiter, *Phys. Rev. B* **76**, 155322 (2007).
- F. Wu, J. Ewing, C. Lynsky, M. Iza, S. Nakamura, S. P. DenBaars, and J. S. Speck, *J. Appl. Phys.* **133**, 035703 (2023).
- Y. Yamaguchi, Y. Kanitani, Y. Kudo, J. Uzuhashi, T. Ohkubo, K. Hono, and S. Tomiya, *Nano Lett.* **22**, 6930 (2022).
- C. H. Ho, J. S. Speck, C. Weisbuch, and Y.-R. Wu, *Phys. Rev. Appl.* **17**, 014033 (2022).
- S. Marcinkevičius, J. Ewing, R. Yapparov, F. Wu, S. Nakamura, and J. S. Speck, *Appl. Phys. Lett.* **123**, 201102 (2023).
- T. Tak, C. W. Johnson, W. Y. Ho, F. Wu, M. Sauty, S. Rebollo, A. K. Schmid, J. Peretti, Y.-R. Wu, C. Weisbuch, and J. S. Speck, *Phys. Rev. Appl.* **20**, 064045 (2023).
- Y. C. Chow, T. Tak, F. Wu, J. Ewing, S. Nakamura, S. P. DenBaars, Y.-R. Wu, C. Weisbuch, and J. S. Speck, *Appl. Phys. Lett.* **123**, 091103 (2023).
- U. Özgür and H. O. Everitt, *Phys. Rev. B* **67**, 155308 (2003).
- R. Ivanov, S. Marcinkevičius, Y. Zhao, D. L. Becerra, S. Nakamura, S. P. DenBaars, and J. S. Speck, *Appl. Phys. Lett.* **107**, 211109 (2015).
- A. Pinos, S. Marcinkevičius, M. Usman, and A. Hallén, *Appl. Phys. Lett.* **95**, 112108 (2009).
- T. K. Uždavinys, S. Marcinkevičius, J. H. Leach, K. R. Evans, and D. C. Look, *J. Appl. Phys.* **119**, 215706 (2016).
- K. Kojima, S. Takashima, M. Edo, K. Ueno, M. Shimizu, T. Takahashi, S. Ishibashi, A. Uedono, and S. F. Chichibu, *Appl. Phys. Express* **10**, 061002 (2017).
- A. Alkauskas, M. D. McCluskey, and C. G. Van de Walle, *J. Appl. Phys.* **119**, 181101 (2016).
- O. Brandt, H. Yang, and K. H. Ploog, *Phys. Rev. B* **54**, R5215 (1996).
- B. Deveaud, J. Shah, T. C. Damen, B. Lambert, and A. Regreny, *Phys. Rev. Lett.* **58**, 2582 (1987).
- V. Liulio, S. Marcinkevičius, Y.-D. Lin, H. Ohta, S. P. DenBaars, and S. Nakamura, *J. Appl. Phys.* **108**, 023101 (2010).
- P. Sčajej, K. Jarašiūnas, S. Okur, U. Özgür, and H. Morkoç, *J. Appl. Phys.* **111**, 023702 (2012).
- U. Penner, H. Rücker, and I. N. Yassievich, *Semicond. Sci. Technol.* **13**, 709 (1998).

- ³⁰R. Shivaraman, Y. Kawaguchi, S. Tanaka, S. P. DenBaars, S. Nakamura, and J. S. Speck, *Appl. Phys. Lett.* **102**, 251104 (2013).
- ³¹H.-M. Solowan, J. Danhof, and U. T. Schwarz, *Jpn. J. Appl. Phys., Part 1* **52**, 08JK07 (2013).
- ³²J. Danhof, H.-M. Solowan, U. T. Schwarz, A. Kaneta, Y. Kawakami, D. Schiavon, T. Meyer, and M. Peter, *Phys. Status Solidi B* **249**, 480 (2012).
- ³³A. David, *Phys. Rev. Appl.* **15**, 054015 (2021).
- ³⁴K. Nomeika, R. Aleksiejūnas, S. Miasojedovas, R. Tomašiūnas, K. Jarašiūnas, I. Pietzonka, M. Strassburg, and H.-J. Lugauer, *J. Lumin.* **188**, 301 (2017).
- ³⁵M. Mensi, R. Ivanov, T. K. Uždavinys, K. M. Kelchner, S. Nakamura, S. P. DenBaars, J. S. Speck, and S. Marcinkevičius, *ACS Photonics* **5**, 528 (2018).